

prolactin-releasing peptide (PrP)-20, PrP-31, sarafotoxin S6a, sarafotoxin S6b, sarafotoxin S6c, secretoneurin, somatostatin 28 (1–12), substance P, thymosin  $\beta$ -10, enterostatin VPDPR, [ $\beta$ -Ala<sup>8</sup>]neurokinin A (4–10), [D-Tyr<sup>6</sup>,  $\beta$ -Ala<sup>11</sup>, Phe<sup>13</sup>, Nle<sup>14</sup>]-Bombesin (6–14), [pGlu]apelin-13, enterostatin APGPR, agouti-related peptide (AGRP) 25–31, AGRP 54–82, AGRP 83–132, YMRP-amide and LPLRF-amide. Human NMU-25 was custom synthesized (Research Genetics). Porcine NMU-8, NMU-25 and rat NMU-25 were purchased from Phoenix Pharmaceuticals. FLIPR assays were performed in COS-7 cells transiently transfected with FM-3/pIRESpuromycin, FM-4/pcDNA3.1 or control vector as described<sup>24</sup>. All transient transfections were carried out using Lipofectamine-2000 (GIBCO-BRL) by following the manufacturer's instructions. We carried out radioligand binding analysis as described<sup>24</sup>. Rat NMU-23 was labelled with [<sup>125</sup>I] at its amino-terminal tyrosine residue (Woods Assay) to a specific activity of ~ 2,000 Ci mmol<sup>-1</sup>.

## Expression analysis

Multi-tissue northern blots (Clontech) and *in situ* hybridization analysis of human NMU1R in monkey intestine was done as described<sup>24</sup>. *In situ* hybridization analysis of NMU2R from rat brain was carried out using <sup>33</sup>P-labelled antisense oligonucleotide probes (equal mix of oligo 420, 5'-AGGAAAGGTAATTGTGGCCACATCTCGTAGAT TTCCA-GAGGCATC-3', and oligo 421, 5'-CACAGTCTCGAAGAGGGCTGCTTTGAA GTAG-CATCCACAGGC-3') as described<sup>26</sup>. Quantitative *in situ* hybridization of NMU and POMC was performed using the same procedure with the NMU probe (5'-TTCTGGTGAATCTTTGAGCGCATATTTGGCGTACCTCTGCAAGC-3') and the POMC probe (5'-CGTCTTGATGATGGCGTCTTGAAGAGCGTCACCAGGGGGC TCT-3').

## Animal studies

Male rats (Charles River Sprague Dawley) weighing 250–350 g were maintained in a temperature and humidity controlled facility with a 12-h light/dark cycle (04:00 lights on). Cannulation and ICV administration were performed essentially as described<sup>27</sup>. Rats were injected ICV with 1, 3 or 10  $\mu$ g of rat NMU-23 (Phoenix Pharmaceuticals). Additional rats were injected ICV with either 0.3 or 0.03  $\mu$ g of MT-II (Peninsula Laboratories) as a positive control for food intake suppression. One group of rats also had a radio transmitter placed in the peritoneal cavity for measurement of core body temperature and gross motor activity (MiniMitter). In the mouse studies we used one-year-old, diet-induced obese (DIO, body fat content 60%) male C57BL/6 mice (Taconic). Mice were ICV-cannulated, injected and monitored for food intake as described above.

In the CTA study, rats were conditioned to 2 h daily access to water, with access to water from two bottles for 2 h each day for 3 days. On the fourth day, rats were given 0.15% saccharin for the 2-h period instead of water and saccharin consumption was measured. Rats were injected with NMU-23 (0, 3 or 10  $\mu$ g, ICV). LiCl was used as a positive control (0.15 M; 2 ml kg<sup>-1</sup>, intraperitoneal (i.p.)). On the fifth day, rats were given saccharin alone for the first hour, then water was added for the remaining 23 h. We measured fluid consumption 1, 2 and 24 h after the injection. In the salt appetite assay, rats were given 0.5 M NaCl salt water to drink for 3 days along with food and regular water. After 3 days, two injections of furosemide (5 mg per 0.2 ml, subcutaneous) were given 1 h apart to sodium-deplete the rats. Rats were then returned to salt-free water and given a sodium-deficient diet. Twenty-four hours after furosemide administration, rats were given NMU (0, 3 or 10  $\mu$ g, ICV), or LiCl (0.15 M, 2 ml kg<sup>-1</sup>, i.p.), and given water and 0.5 M NaCl to drink. Fluid consumption was measured 1, 2 and 24 h after dosing.

All rodent studies were conducted in accord with rules and guidelines of the Merck Research Laboratories Institutional Animal Care and Use Committee and the NIH Guidelines for the Care and Use of Laboratory Animals.

Received 16 March; accepted 17 May 2000.

1. Minamino, N., Kangawa, K. & Matsuo, H. Neuromedin U-8 and U-25: novel uterus stimulating and hypertensive peptides identified in porcine spinal cord. *Biochem. Biophys. Res. Commun.* **130**, 1078–1085 (1985).
2. Domin, J., Ghatei, M. A., Chohan, P. & Bloom, S. R. Characterization of neuromedin U like immunoreactivity in rat, porcine, guinea-pig and human tissue extracts using a specific radio-immunoassay. *Biochem. Biophys. Res. Commun.* **140**, 1127–1134 (1986).
3. Conlon, J. M. *et al.* Primary structure of neuromedin U from the rat. *J. Neurochem.* **51**, 988–991 (1988).
4. Minamino, N., Kangawa, K., Honzawa, M. & Matsuo, H. Isolation and structural determination of rat neuromedin U. *Biochem. Biophys. Res. Commun.* **156**, 355–360 (1988).
5. Domin, J. *et al.* The distribution, purification, and pharmacological action of an amphibian neuromedin U. *J. Biol. Chem.* **264**, 20881–20885 (1989).
6. O'Harte, F. *et al.* Primary structure and pharmacological activity of a nonapeptide related to neuromedin U isolated from chicken intestine. *Peptides* **12**, 809–812 (1991).
7. Kage, R., O'Harte, F., Thim, L. & Conlon, J. M. Rabbit neuromedin U-25: lack of conservation of a posttranslational processing site. *Regul. Pept.* **33**, 191–198 (1991).
8. Domin, J., Benito-Orfila, M. A., Nandha, K. A., Aitken, A. & Bloom, S. R. The purification and sequence analysis of an avian neuromedin U. *Regul. Pept.* **41**, 1–8 (1992).
9. Honzawa, M., Sudoh, T., Minamino, N., Tohyama, M. & Matsuo, H. Topographic localization of neuromedin U-like structures in the rat brain: an immunohistochemical study. *Neuroscience* **23**, 1103–1122 (1987).
10. Ballesta, J. *et al.* Occurrence and developmental pattern of neuromedin U-immunoreactive nerves in the gastrointestinal tract and brain of the rat. *Neuroscience* **25**, 797–816 (1988).
11. Brown, D. R. & Quito, F. L. Neuromedin U octapeptide alters ion transport in porcine jejunum. *Eur. J. Pharmacol.* **155**, 159–162 (1988).
12. Sumi, S. *et al.* Effect of synthetic neuromedin U-8 and U-25, novel peptides identified in porcine

- spinal cord, on splanchnic circulation in dogs. *Life Sci.* **41**, 1585–1590 (1987).
13. Gardiner, S. M., Compton, A. M., Bennett, T., Domin, J. & Bloom, S. R. Regional hemodynamic effects of neuromedin U in conscious rats. *Am. J. Physiol.* **258**, R32–38 (1990).
14. Malendowicz, L. K. *et al.* Effects of neuromedin U (NMU)-8 on the rat hypothalamo-pituitary-adrenal axis. Evidence of a direct effect of NMU-8 on the adrenal gland. *Neuropeptides* **26**, 47–53 (1994).
15. Tan, C. P. *et al.* Cloning and characterization of a human and murine T-cell orphan G-protein-coupled receptor similar to the growth hormone secretagogue and neurotensin receptors. *Genomics* **52**, 223–229 (1998).
16. Retief, J. D., Lynch, K. R. & Pearson, W. R. Panning for genes—A visual strategy for identifying novel gene orthologs and paralogs. *Genome Res.* **9**, 373–382 (1999).
17. Brady, L. S., Smith, M. A., Gold, P. W. & Herkenham, M. Altered expression of hypothalamic neuropeptide mRNAs in food-restricted and food-deprived rats. *Neuroendocrinology* **52**, 441–447 (1990).
18. Kristensen, P. *et al.* Hypothalamic CART is a new anorectic peptide regulated by leptin. *Nature* **393**, 72–76 (1998).
19. Zhang, Y. *et al.* Positional cloning of the mouse obese gene and its human homologue. *Nature* **372**, 425–432 (1994).
20. Chavez, M., Seeley, R. J. & Woods, S. C. A comparison between effects of intraventricular insulin and intraperitoneal lithium chloride on three measures sensitive to emetic agents. *Behav. Neurosci.* **109**, 547–550 (1995).
21. Stricker, E. M. & Verbalis, J. G. in *Handbook of Behavioural Neurobiology of Food and Fluid Intake* (ed. Stricker, E. M.) 45–60 (Plenum, New York, 1990).
22. Kissileff, H. R. Food-associated drinking in the rat. *J. Comp. Physiol. Psychol.* **67**, 284–300 (1969).
23. Button, D. & Brownstein, M. Aequorin-expressing mammalian cell lines used to report Ca<sup>2+</sup> mobilization. *Cell. Calcium* **14**, 663–671 (1993).
24. Liu, Q. *et al.* Identification of urotensin II as the endogenous ligand for the orphan G-protein-coupled receptor GPR14. *Biochem. Biophys. Res. Commun.* **266**, 174–178 (1999).
25. Unguin, M. D., Singh, L. M., Stocco, R., Sas, D. E. & Abramovitz, M. An automated aequorin luminescence-based functional calcium assay for G-protein-coupled receptors. *Anal. Biochem.* **272**, 34–42 (1999).
26. Guan, X. M., Yu, H. & Van der Ploeg, L. H. Evidence of altered hypothalamic pro-opiomelanocortin/neuropeptide Y mRNA expression in tubby mice. *Brain Res. Mol. Brain Res.* **59**, 273–279 (1998).
27. Murphy, B. *et al.* Melanocortin mediated inhibition of feeding behavior in rats. *Neuropeptides* **32**, 491–497 (1998).

## Acknowledgements

We thank M. Abramovitz and R. Stocco of Merck Frosst Canada for setting up the aequorin assay.

Correspondence and requests for materials should be addressed to Q.L. (e-mail: Jim\_liu@merck.com). The GenBank accession numbers are human FM-3/GPR66 (NM\_006056), rat FM-3 (AF242873), human FM-4 (AF242874) and rat FM-4 (AF242875).

# Initiation of neural induction by FGF signalling before gastrulation

Andrea Streit\*, Alyson J. Berliner†, Costis Papanayotou\*, Andrés Sirulnik\* & Claudio D. Stern\*†

\* Department of Genetics and Development and † Center for Neurobiology and Behavior, Columbia University, 701 West 168th Street #1602, New York, New York 10032, USA

During neural induction, the 'organizer' of the vertebrate embryo instructs neighbouring ectodermal cells to become nervous system rather than epidermis. This process is generally thought to occur around the mid-gastrula stage of embryogenesis<sup>1</sup>. Here we report the isolation of *ERNI*, an early response gene to signals from the organizer (Hensen's node). Using *ERNI* as a marker, we present evidence that neural induction begins before gastrulation—much earlier in development than previously thought. We show that the organizer and some of its precursor cells produce a fibroblast growth factor signal, which can initiate, and is required for, neural induction.

The prevailing model for neural induction suggests that cells differentiate into neural fates by default, but are normally inhibited by bone morphogenetic proteins (BMPs). The organizer, by emitting BMP antagonists, allows cells in its vicinity to execute their default neural programme<sup>2,3</sup>. However, other work suggests a more

complex mechanism<sup>4-7</sup>. In the chick embryo, naive epiblast cells do not respond to BMP antagonists unless previously exposed to organizer signals for five hours<sup>4</sup>. We have therefore designed a differential screen for genes that are induced in the epiblast by a grafted organizer within this time period. Among the complementary DNAs isolated is the gene *ERNI* (for early response to neural induction); it is not homologous to any known sequence and contains a putative coiled-coil domain and tyrosine phosphorylation site (Fig. 1a). When transfected into COS cells, ERNI protein is found throughout the cytoplasm in most cells (Fig. 1b), but is restricted to the nucleus in about 10% of cells, which are invariably smaller and fibroblast-like (Fig. 1c). The predicted structure and subcellular localization suggests that ERNI could be part of a protein complex that travels from the cytoplasm to the nucleus.

Induction is defined as "an interaction between two tissues, as a result of which the responding cells change their fate"<sup>8</sup>. To ensure that the responses to the grafted organizer are due to induction, rather than recruitment of cells from the neural plate, the screen was designed using the extra-embryonic region, which does not normally contribute to the nervous system<sup>9</sup>. Therefore any gene identified in this screen that is relevant to neural induction should be expressed at some stage in the prospective neural plate of the normal embryo. Indeed, we find that *cERNI* begins to be expressed at pre-primitive streak stages, throughout the region that will contribute to the nervous system<sup>10</sup> (Fig. 2a); by streak stages (3<sup>+</sup>/4), its distribution coincides with the known limits of the prospective neural plate<sup>11</sup> (Fig. 2b). Shortly thereafter, expression clears from the centre of the neural plate and becomes confined to its border (Fig. 2c); transcripts disappear by early somite stages. A quail Hensen's node (stage 3<sup>+</sup>/4) induces *cERNI* expression in chick extra-embryonic epiblast in as little as 1–2 h (25/25). By 5h *cERNI* induction is most intense (20/20; Fig. 2d), and by 8h it begins to clear from the centre (26/26), forming a ring resembling its normal

expression at the border of the neural plate. These findings make *cERNI* the earliest known marker for a response to organizer signals, even earlier than *Sox3* (whose early expression it resembles and which is induced by the node in 3 h (ref. 12); Fig. 3d).

Which signalling molecules from the organizer are responsible for inducing *cERNI*? One approach to identifying candidate factors is to assess the ability of embryonic tissues to induce *cERNI*, to map the distribution of inducing factors. Head process (stage 5–6; 2/2), notochord (stage 10; 6/6), prechordal mesendoderm (stage 5; 14/14) and presomitic mesoderm (stage 10; 19/19) all induce *cERNI*, whereas other tissues tested have either reduced (somites, 8/21; posterior primitive streak, 9/23) or no ability to generate ectopic *cERNI* expression (lateral mesoderm, 0/6; stage 4–5 neural plate, 0/17; stage 10 neural tube, 1/5; area opaca, 0/10). This distribution of inducing ability is reminiscent of sites of fibroblast growth factor (FGF) activity<sup>13</sup>. Indeed, FGF8-coated beads induce *cERNI* expression as strongly and as quickly as does the node, within 1–2 h (19/20; Fig. 2f), without inducing the mesodermal markers *brachyury* (0/8) or *Tbx6L* (0/6) (see also ref. 14). In contrast, ectopic expression of *cERNI* was never observed after misexpression of the BMP antagonists chordin (0/21), *noggin* (0/17) or *cerberus* (0/18), or of *BMP4* (0/15) or hepatocyte growth factor/scatter factor (*HGF/SF*) (0/21). FGF8 also strongly induces the expression of *Sox3*, but not the later neural marker *Sox-2* (ref. 12). Together, these findings implicate FGFs as possible early signals in the neural induction cascade. Of the members of this family, FGF8 is the best candidate endogenous inducer because at primitive streak stages it is expressed in the anterior part of the streak including the node, and is downregulated as the node begins to lose neural inducing ability<sup>12</sup>.

Is FGF expression in Hensen's node required to induce *cERNI* and *Sox3*? We used two different loss-of-function approaches: the FGF-receptor inhibitor SU5402, which specifically interferes with the FGF signalling pathway<sup>15</sup>, and cells secreting the extracellular

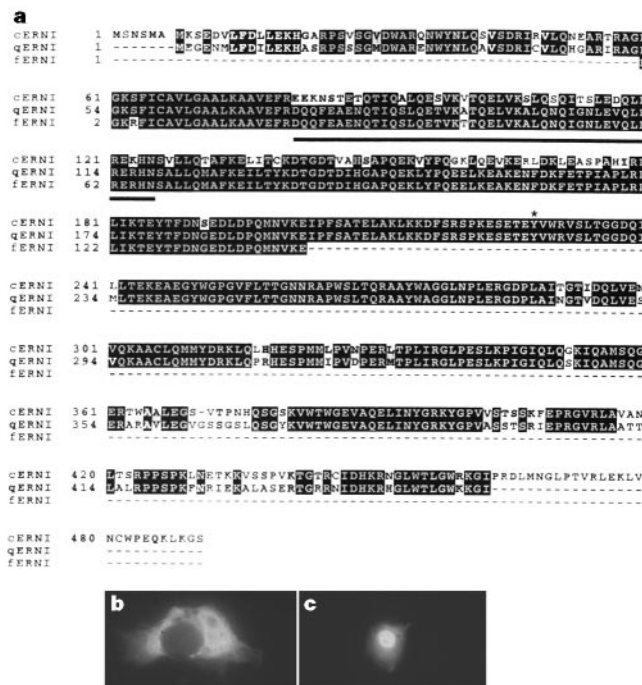


**Figure 1** Structure and cellular localization of ERNI. **a**, Alignment of amino-acid sequences of chick, quail and zebrafinch *ERNI*. Chick *ERNI* shows an open reading frame of 1,470 bp encoding a 490-amino-acid protein. A coiled-coil domain (underlined) is predicted by MULTICOIL ( $P = 1$ ) and PAIRCOIL ( $P = 0.997$ ). Position 228 (asterisk) is a putative tyrosine phosphorylation site. The partial quail and zebrafinch cDNAs show

overall amino-acid identity of 82% and 72% to *cERNI*, respectively. **b, c**, Subcellular localization of ERNI protein visualized by immunofluorescence after transfection of COS cells with myc-tagged *cERNI*. In most cells ERNI was detected in the cytoplasm (**b**), but a subset of cells showed nuclear localization (**c**).

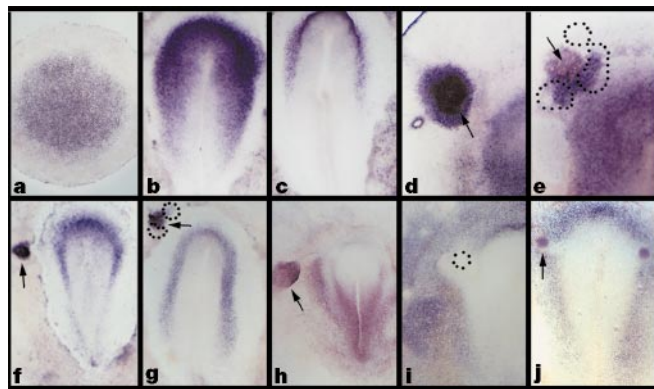


**Figure 2** *cERNI* expression in the neural plate and its induction by Hensen's node and FGF8. *cERNI* is expressed in the prospective neural plate<sup>12,13</sup> of embryos at the pre-primitive streak (a) and primitive streak (b) stage. It becomes restricted to the border at head-fold stages (c). Both Hensen's node (d, e; brown, arrow) and FGF8 (f, g; arrow) strongly induce *cERNI* expression, even in the presence of excess BMP4 (secreting cells outlined). FGF8 differentially regulates the expression of some BMP targets: it induces expression of *msx-1* within 3 h (h), but represses expression of the non-neural markers *GATA-2* (i) and -3 (j). Arrows in h and j and outline in i mark FGF8 beads.

portion of the FGF receptor<sup>16</sup>. SU5402 greatly reduced the frequency of induction by a grafted node of *Sox3* (from 16/16 in controls to 1/15—a 93% reduction; 5 h incubation; Fig. 3e) and of *cERNI* (from 20/20 in controls to 20/30—a 33% reduction in frequency; in the remaining embryos the intensity of expression was reduced; 3 h incubation; Fig. 3b). Moreover, cells secreting chimaeric FGF receptor markedly reduced induction by the node of *Sox3* (0/8; Fig. 3f) and of *cERNI* (6/38—83% reduction; Fig. 3c), whereas in the presence of control cells both genes were induced in 100% of cases ( $n = 16$ ; Fig. 3a, d). We also noticed a marked reduction in the level of expression of both *cERNI* and *Sox3* in the normal neural domain of the host embryo in the presence of FGF inhibitors (compare Fig. 3k and j).

To investigate whether later steps of neural induction also depend on FGF signalling, we grafted quail nodes together with SU5402 beads into the area opaca of chick hosts. After overnight incubation (16 h), *Sox2* induction by the node was reduced to 20% (4/20; Fig. 3g, h) when compared with controls (10/10; Fig. 3g, i). The nodes, however, elongated normally and continued to express the organizer marker *chordin* (10/11; Fig. 3g–i), showing that the graft itself remains unaffected by the FGF inhibitor. These experiments strongly implicate FGF signalling as an essential component of the neural induction pathway initiated by the organizer.

In other systems, FGF and BMP signalling pathways can synergize or antagonize each other. We therefore investigated the effect of FGF8 on the expression of the BMP targets *msx1*, *GATA2* and *GATA3*. FGF8 induces *msx1* expression in 3 h (5/5; Fig. 2h), but represses expression of the non-neural markers *GATA2* (4/5; Fig. 2i) and -3 (4/6; Fig. 2j) in 5–6 h. The possibility remains that the ability of the node to induce *cERNI* and *Sox3* still requires BMP inhibition. To test this, we grafted stage 3<sup>+</sup>/4 nodes, or FGF8 beads, into host embryos together with cells secreting BMP4. Even in the presence of excess BMP4, both the node (Fig. 2e) and FGF8 (Fig. 2f) continued to induce *cERNI* (13/14 nodes; 10/12 FGF8) and *Sox3* (12/14 nodes; 6/8 FGF8). Together, these results suggest that the activity of FGF8 is complex, and cannot be explained merely through antagonism of the BMP pathway.

Both *cERNI* (Fig. 2a) and *Sox3* start to be expressed long before gastrulation, raising the possibility that the initial steps of neural induction could begin this early. At this stage, the organizer has not yet formed, but two cell populations that will contribute to it have been defined (Fig. 4a). The first is a group of middle layer cells

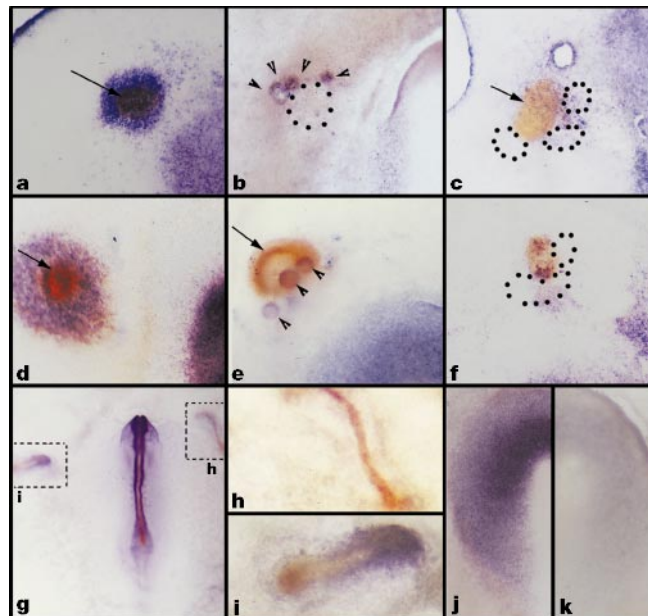


**Figure 3** FGF signalling is an essential component of the neural induction pathway. Hensen's node (brown) induces *cERNI* (a, arrow), *Sox3* (d, arrow) and *Sox2* (left in g, i). The FGF receptor inhibitor SU5402 (arrowheads in b, e) inhibits induction of all three genes (b, e; right in g, h) by the node, which still elongates and expresses the organizer marker *chordin* (g–i; *Sox2* in purple, *chordin* in red). Cells secreting a soluble form of the FGF receptor (outlined) also greatly reduce induction of *cERNI* (c) and *Sox3* (f) by the node. The endogenous expression of *Sox3* is reduced in embryos treated with SU5402 (k) as compared with untreated embryos (j) (embryos processed simultaneously in the same vial).

associated with Koller's sickle (hereafter referred to as 'posterior cells'), which later moves to the centre of the embryo with the tip of the elongating primitive streak (stages 2–3)<sup>17</sup>. The second population, hereafter referred to as 'central cells', is located in the epiblast overlying the posterior cells until stage X, but moves to the centre of the area pellucida before primitive streak formation begins (stages XI–XIII)<sup>10</sup>. Hensen's node is formed when the two populations come together. We investigated the inducing ability of these two populations of organizer precursors, alone or in combination. Chick central cells grafted into the area opaca of a stage 3<sup>+</sup>/4 quail host do not induce *qERNI* (0/4), *Sox3* (0/17), *Sox2* (0/6) or the organizer marker *chordin* (0/5). In contrast, chick posterior cells induce *qERNI* (21/21; Fig. 4d) and *Sox3* (8/11; Fig. 4e) strongly after 5 h, but not the later neural marker *Sox2* or *chordin* (both after 16h;  $n = 10$ ). A combination of central and posterior cells induces both *Sox2* (3/5; Fig. 4f) and *chordin* (3/5; Fig. 4g) after overnight culture; other regions of area pellucida epiblast cannot substitute for the central cells in this assay ( $n = 7$ ). These findings show that posterior, but not central cells, induce *ERNI* and *Sox3*. A combination of the two generates a functional organizer, as well as expression of the later neural marker *Sox2*.

Where is FGF8 expressed at these early stages? A stage X, the posterior cells, but not central cells, express FGF8 (Fig. 4b). As the hypoblast starts to form from the posterior margin, it also expresses FGF8, albeit at low level (Fig. 4c). By stage XIII, the domain of *cERNI* and *Sox3* expression in the epiblast mirrors the area covered by hypoblast. Consistent with these expression patterns, grafts of hypoblast into the area opaca of stage 3<sup>+</sup> hosts induce *cERNI* within 3 h (4/4; not shown). Is the inducing ability of posterior cells due to FGF? In the presence of the FGF inhibitor SU5402, induction of both *ERNI* (0/5) and *Sox3* (0/5) by posterior cells is abolished.

Our findings suggest that neural induction is initiated before the



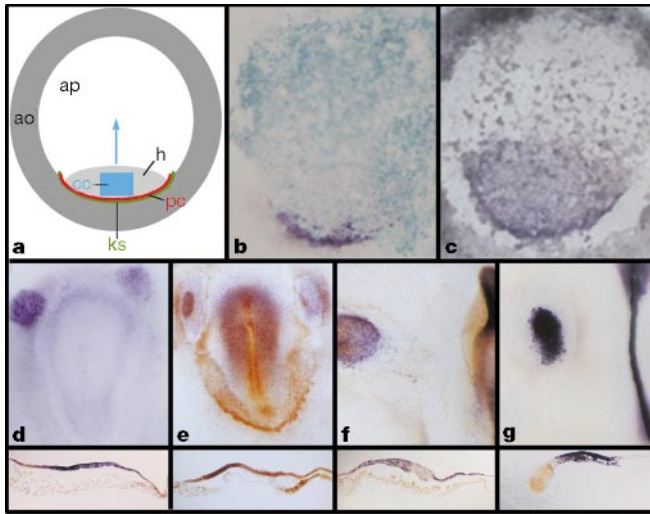


**Figure 4** Organizer precursor cells initiate the neural induction cascade. **a**, Diagram showing the position of the two organizer precursor cell populations (pc and cc) at stage XI. ao, area opaca; ap, area pellucida; h, hypoblast; ks, Koller's sickle; pc, posterior cells; cc, central cells. The arrow indicates the movement of central cells occurring at stages XI–XIII. **b**, At stage X, *FGF8* is expressed in the posterior cells and subsequently (**c**; stage XII) in the forming hypoblast. *cERN1* (**d**) and *Sox3* (**e**) are strongly induced by posterior cells, whereas induction of *Sox2* (**f**) and *chordin* (**g**) requires signals from both organizer precursor populations. Insets below **d–g** show sections of the grafts in **d–g**, respectively. Quail embryos were used as hosts in **d, e** and as donors in **f, g** (in both cases quail cells labelled by QCPN, brown).

beginning of gastrulation by FGF emanating from a population of organizer precursors at the posterior margin of the embryo (perhaps reinforced by the spreading hypoblast). The coming together of this cell population with a second precursor population in the epiblast generates a fully functional organizer that provides the remaining signals in a cascade, including BMP antagonists. These results provide an explanation for the hitherto unexplained finding that in *Xenopus*, BMP antagonists do not induce neural tissue in the presence of dominant-negative FGF receptors<sup>18,19</sup> and for controversial reports of FGF as a direct neural inducer<sup>20–23</sup>. FGF signals are clearly not sufficient to generate a complete nervous system. But are they sufficient to sensitize the epiblast to BMP antagonists and to generate expression of later neural markers? The finding that *msx1* is upregulated by FGF8 raises the possibility that this is part of a mechanism that leads to self-maintaining activation of BMP signalling<sup>12,24</sup>, which would be a required first step if the BMPs are later to be inhibited. On the other hand, neither FGF nor 5 h of signals from the node followed by BMP antagonists is sufficient to generate induction of *Sox2* or later neural markers<sup>4,12</sup>. We propose that neural induction is a multi-step process of considerable complexity. FGF mimics the first 5 h of signals from the organizer, but further steps remain to be discovered. □

## Methods

### Differential screen

A quail node (stage 3<sup>+</sup>) was grafted into the area opaca of a chick host; after 5 h the epiblast that had been in contact with it was dissected ('induced epiblast'). A similar piece of tissue was isolated from the contralateral side of the same embryo ('uninduced epiblast'). From each tissue cDNA was generated from 10 different cell populations (10–15 cells) and libraries were constructed<sup>25</sup>. One cDNA preparation was selected from each tissue; both had similar levels of the ubiquitously expressed ribosomal gene *S17*, whereas the early neural marker *Sox3* was present only in the induced tissue. The library from induced tissue was plated at low density and differentially screened using radioactively labelled total cDNA from both cell populations. Of 38 differentially expressed cDNAs, 36 corresponded to *cERN1*. A full-length clone (GenBank AF218814) was isolated by screening a chick gastrula-stage library. The full-length cDNA encodes a transcript of 4.5 kilobases (kb), which was confirmed by northern blot (not shown).

A quail primitive-streak-stage cDNA library was screened at low stringency to isolate a

quail *ERN1* homologue (GenBank AF218815). Zebrafish *ERN1* was isolated by genomic polymerase chain reaction (PCR) using degenerate primers, which amplified a 366-base pair (bp) fragment (*fERN1*).

### Embryo culture and grafting

Fertile hens' eggs (White Leghorn, Spafas) and quails' eggs (Strickland) were incubated at 38 °C for 1–38 h to yield embryos at stages XI (ref. 26) to 10 (ref. 27). Host embryos (chick or quail) were maintained in New culture<sup>28</sup>. Donor nodes from stage 3<sup>+</sup> were transplanted to the inner margin of the area opaca of a host of the same stage. Organizer precursor cells (Fig. 4a) were mostly isolated from chick embryos where the fate maps are more complete<sup>10,17</sup>. Posterior cells and associated Koller's sickle were dissected using syringe needles and transplanted to the area opaca of a quail host (stage 3<sup>+</sup>/4). To isolate central cells, hypoblast was removed and a square of epiblast (150 µm) excised.

FGF8-coated heparin beads were prepared as described<sup>12</sup>. Chordin, Noggin, cerberus and BMP4-expressing cells were generated and grafted as described<sup>4,29</sup>. Expression levels were routinely checked by immunostaining and immunoblots. To interfere with FGF signalling, pellets of 2,000–3,000 cells expressing a fusion protein of the extracellular domain of FGFR1 and rat IgG2a<sup>16</sup> were grafted together with Hensen's node. AG1X2 beads were coated with 25 µM SU5402 (Calbiochem) in PBS for 1–2 h, washed and grafted together with the node or posterior cells into a host that had been pre-incubated briefly in inhibitor (2.5 µM).

### Whole mount *in situ* hybridization and immunocytochemistry

Whole mount *in situ* hybridization and QCPN antibody staining were performed as described<sup>19,30</sup>.

Received 14 March; accepted 3 May 2000.

- Harland, R. & Gerhart, J. Formation and function of Spemann's organizer. *Annu. Rev. Cell Dev. Biol.* **13**, 611–667 (1997).
- Wilson, P. A. & Hemmati-Brivanlou, A. Vertebrate neural induction: inducers, inhibitors, and a new synthesis. *Neuron* **18**, 699–710 (1997).
- Schier, A. F. & Talbot, W. S. The zebrafish organizer. *Curr. Opin. Genet. Dev.* **8**, 464–471 (1998).
- Streit, A. *et al.* Chordin regulates primitive streak development and the stability of induced neural cells, but is not sufficient for neural induction in the chick embryo. *Development* **125**, 507–519 (1998).
- Baker, J. C., Beddington, R. S. & Harland, R. M. Wnt signaling in *Xenopus* embryo inhibits BMP4 expression and activates neural development. *Genes Dev.* **13**, 3149–3159 (1999).
- Klingensmith, J., Ang, S. L., Bachiller, D. & Rossant, J. Neural induction and patterning in the mouse in the absence of the node and its derivatives. *Dev. Biol.* **216**, 535–549 (1999).
- Streit, A. & Stern, C. D. Neural induction. A bird's eye view. *Trends Genet.* **15**, 20–24 (1999).
- Gurdon, J. B. Embryonic induction—molecular prospects. *Development* **99**, 285–306 (1987).
- Streit, A. *et al.* Preventing the loss of competence for neural induction: HGF/SF, L5 and Sox-2. *Development* **124**, 119–1202 (1997).
- Hatada, Y. & Stern, C. D. A fate map of the epiblast of the early chick embryo. *Development* **120**, 2879–2889 (1994).
- Garcia-Martinez, V., Alvarez, I. S. & Schoenwolf, G. C. Locations of the ectodermal and nonectodermal subdivisions of the epiblast at stages 3 and 4 of avian gastrulation and neurulation. *J. Exp. Zool.* **267**, 431–446 (1993).
- Streit, A. & Stern, C. D. Establishment and maintenance of the border of the neural plate in the chick: involvement of FGF and BMP activity. *Mech. Dev.* **82**, 51–66 (1999).
- Chambers, D. & Mason, I. Expression of sprouty-2 during early development of the chick embryo is coincident with known sites of FGF signalling. *Mech. Dev.* **91**, 361–364 (2000).
- Storey, K. G. *et al.* Early posterior neural tissue is induced by FGF in the chick embryo. *Development* **125**, 473–484 (1998).
- Mohammadi, M. *et al.* Structures of the tyrosine kinase domain of fibroblast growth factor receptor in complex with inhibitors. *Science* **276**, 955–960 (1997).
- Ye, W., Shimamura, K., Rubenstein, J. L., Hynes, M. A. & Rosenthal, A. FGF and Shh signals control dopaminergic and serotonergic cell fate in the anterior neural plate. *Cell* **93**, 755–759 (1993).
- Izpisua-Belmonte, J. C., De Robertis, E. M., Storey, K. G. & Stern, C. D. The homeobox gene gooseoid and the origin of organizer cells in the early chick blastoderm. *Cell* **74**, 645–659 (1993).
- Launay, C., Fromentoux, V., Shi, D. L. & Boucaut, J. C. A truncated FGF receptor blocks neural induction by endogenous *Xenopus* inducers. *Development* **122**, 869–880 (1996).
- Sasai, Y., Lu, B., Piccolo, S. & De Robertis, E. M. Endoderm induction by the organizer-secreted factors chordin and noggin in *Xenopus* animal caps. *EMBO J.* **15**, 4547–4555 (1996).
- Amaya, E., Musci, T. J. & Kirschner, M. W. Expression of a dominant negative mutant of the FGF receptor disrupts mesoderm formation in *Xenopus* embryos. *Cell* **66**, 257–270 (1991).
- Lamb, T. M. & Harland, R. M. Fibroblast growth factor is a direct neural inducer, which combined with noggin generates anterior–posterior neural pattern. *Development* **121**, 3627–3636 (1995).
- Alvarez, I. S., Araujo, M. & Nieto, M. A. Neural induction in whole chick embryo cultures by FGF. *Dev. Biol.* **199**, 42–54 (1998).
- Hongo, I., Kengaku, M. & Okamoto, H. FGF signaling and the anterior neural induction in *Xenopus*. *Dev. Biol.* **216**, 561–581 (1999).
- Biehs, B., Francois, V. & Bier, E. The *Drosophila* short gastrulation gene prevents Dpp from autoactivating and suppressing neurogenesis in the neuroectoderm. *Genes Dev.* **10**, 2922–2934 (1996).
- Dulac, C. & Axel, R. A novel family of genes encoding putative pheromone receptors in mammals. *Cell* **83**, 195–206 (1995).
- Eyal-Giladi, H. & Kochav, S. From cleavage to primitive streak formation: a complementary normal table and a new look at the first stages of the development of the chick. I. General morphology. *Dev. Biol.* **49**, 321–337 (1976).
- Hamburger, V. & Hamilton, H. L. A series of normal stages in the development of the chick embryo. *J. Morphol.* **88**, 49–92 (1951).
- Stern, C. D. & Ireland, G. W. An integrated experimental study of endoderm formation in avian embryos. *Anat. Embryol.* **163**, 245–263 (1981).

29. Streit, A. & Stern, C. D. Mesoderm patterning and somite formation during node regression: differential effects of chordin and noggin. *Mech. Dev.* **85**, 85–96 (1999).  
 30. Stern, C. D. Detection of multiple gene products simultaneously by in situ hybridization and immunohistochemistry in whole mounts of avian embryos. *Curr. Top. Dev. Biol.* **36**, 223–243 (1998).

**Acknowledgements**

We thank A. Rosenthal and W. Ye (Genentech) for the FGFR1-IgG construct; R. Lovell-Badge for *Sox3* and *Sox2* and T. Jessell for S17; C. Dulac for advice on the differential screen; B. Cigich for technical assistance; I. Skromne for Fig. 4b, c; C. Ang for zebrafinch tissue; and T. Jessell, G. Sheng, K. Storey and D. Vasiliaskas for helpful comments on the manuscript. Supported by the National Institute of Mental Health.

Correspondence and requests for materials should be addressed to C.D.S. (e-mail: cds20@columbia.edu).

**Point mutation in an AMPA receptor gene rescues lethality in mice deficient in the RNA-editing enzyme ADAR2**

Miyoko Higuchi\*, Stefan Maas\*†‡, Frank N. Single\*†, Jochen Hartner\*, Andrei Rozov§, Nail Burnashev§, Dirk Feldmeyer§, Rolf Sprengel\* & Peter H. Seeburg\*

\* Departments of Molecular Neurobiology and § Cell Physiology, Max-Planck Institute for Medical Research, Jahnstrasse 29, 69120 Heidelberg, Germany

† These authors contributed equally to this work

RNA editing by site-selective deamination of adenosine to inosine<sup>1,2</sup> alters codons<sup>3,4</sup> and splicing<sup>5</sup> in nuclear transcripts<sup>6</sup>, and therefore protein function. ADAR2 (refs 7, 8) is a candidate mammalian editing enzyme that is widely expressed in brain and other tissues<sup>7</sup>, but its RNA substrates are unknown. Here we have studied ADAR2-mediated RNA editing by generating mice that are homozygous for a targeted functional null allele. Editing in *ADAR2*<sup>-/-</sup> mice was substantially reduced at most of 25 positions in diverse transcripts<sup>3–6</sup>; the mutant mice became prone to seizures and died young. The impaired phenotype appeared to result entirely from a single underedited position, as it reverted to normal when both alleles for the underedited transcript were substituted with alleles encoding the edited version exonically<sup>9</sup>. The critical position specifies an ion channel determinant<sup>10</sup>, the Q/R site<sup>3,6</sup>, in AMPA (α-amino-3-hydroxy-5-methyl-4-isoxazole propionate) receptor<sup>10</sup> GluR-B pre-messenger RNA. We conclude that this transcript is the physiologically most important substrate of ADAR2.

Mammalian transcripts that are known to be edited by site-selective adenosine deamination are expressed largely in brain: most encode subunits of ionotropic glutamate receptors (GluRs) that mediate fast excitatory neurotransmission<sup>3,10</sup>. The only position edited to nearly 100% is the Q/R site of GluR-B, for which the mRNA contains an arginine (R) codon (CIG) in place of the genomic glutamine (Q) codon (CAG)<sup>3</sup>. The physiological importance of this codon substitution wrought by RNA editing was revealed by early onset epilepsy and premature death of mice heterozygous for an intron-11-modified *GluR-B*<sup>ΔECS</sup> allele with Q/R site-uneditable transcripts<sup>11,12</sup>.

Three mammalian adenosine deaminases acting on RNA

(ADAR1–ADAR3; refs 7, 8, 13) form a small family of candidate RNA-editing enzymes that operate on nuclear transcripts. Only ADAR2 edits the Q/R site in GluR-B pre-mRNA efficiently *in vitro*<sup>7,14,15</sup>. Because ADAR2 is expressed in tissues other than brain<sup>7</sup>, distinct pre-mRNAs in different tissues may be substrates for this enzyme. To determine whether ADAR2 edits the Q/R site in GluR-B pre-mRNA *in vivo*, and to evaluate the general physiological significance of ADAR2-mediated RNA editing, we generated mice with functional null alleles for this enzyme.

A targeting vector for functional *ADAR2* gene ablation (Fig. 1a, b) was constructed by replacing most of exon 4 (ref. 16) with a *PGK-neo* gene; exon 4 encodes an essential adenosine deaminase motif<sup>3,7</sup>. Chimaeric mice were generated by injection of a targeted embryonic stem (ES) cell clone<sup>17</sup> into C57BL/6-derived blastocysts. *ADAR2*<sup>+/-</sup> intercrosses produced *ADAR2*<sup>-/-</sup> mice at Mendelian frequency, indicating that ADAR2 deficiency does not interfere with embryonic development. We found residual expression from the targeted *ADAR2*<sup>-</sup> allele through exon skipping, potentially leading to a truncated, enzymatically inactive ADAR2 form with intact RNA-binding domains (Fig. 1c). The expression of this truncated form might amount to less than 10% of ADAR2 in wild-type mice, as predicted from the severely reduced mutant transcript levels (mean ± s.d., 8 ± 3% of wild type, *n* = 3; postnatal day 14 (P14)) determined by ribonuclease (RNase) protection (Fig. 1d).

Heterozygous *ADAR2*<sup>+/-</sup> mice were phenotypically normal, but *ADAR2*<sup>-/-</sup> mice died between P0 and P20 and became progressively seizure-prone after P12, akin to *GluR-B*<sup>+ΔECS</sup> mice<sup>11,12</sup>. Thus, we first studied the effect of ADAR2 deficiency on Q/R site editing of GluR-B pre-mRNA, the substrate for a nuclear RNA-dependent

**Table 1 ADAR2 deficiency and site-selective adenosine deamination**

Editing sites	ADAR2 <sup>+/+</sup>	ADAR2 <sup>+/-</sup>	ADAR2 <sup>-/-</sup>
GluR-B pre-mRNA			
Q/R*	98 ± 3	90 ± 3	10 ± 3
Hotspot1*†	50	45	60
Hotspot2*†‡			
+262	30	20	<10
+263	65	55	<10
+264	15	10	<5
GluR-B mRNA			
Q/R*	100 ± 1	100 ± 1	40 ± 4
AMPA-R† R/G§			
GluR-B	75	55	15
GluR-C	90	85	75
GluR-D	45	40	10
GluR5			
Q/R	64 ± 5	55 ± 2	40 ± 1
GluR6			
Q/R	86 ± 4	78 ± 4	29 ± 8
I/V	87 ± 2	79 ± 7	22 ± 5
Y/C	90 ± 4	82 ± 5	2 ± 1
5HT2C-R†			
A	75	70	70
B	80	75	30
C	15	10	<5
D	70	55	<5
ADAR2†‡			
-1	15	10	<10
+23	25	15	<10
+24	45	35	10

The editing sites have been described<sup>2–5,27</sup>. Values, given as mean ± s.d. (*n* = 3), indicate the percentage of the edited version for the different editing sites analysed in the three genotypes. Values were obtained from whole-brain RNA by differential oligonucleotide-mediated hybridization of cloned RT-PCR products to distinguish between an adenosine (unedited) and a guanosine (edited) at the individual editing sites.

\* Values from P14 mice with unmodified *GluR-B* alleles. All other values were from P40 mice with *GluR-B* alleles sequence modified at the Q/R site codon<sup>9</sup>.

† Values derived from the different peak heights for the two nucleotides in identical positions in DNA sequence chromatograms. Values from three mice were averaged and rounded to the nearest 5 or 0 position in each case.

‡ Sites +265 in hotspot2 and -2, +9 and +10 in ADAR2 were edited to <5% in wild type.

§ Flip and flop splice versions. As assessed from sequence chromatograms, the approximate representations of the flip forms were 50% for GluR-B, 75% for GluR-C and 65% for GluR-D; see ref. 27.

‡ Present address: Department of Biology, Massachusetts Institute of Technology, 77 Massachusetts Avenue, MA 02139, USA.